

Toward Mass Customization Through Additive Manufacturing: An Automated Design Pipeline for Respiratory Protective Equipment Validated Against 205 Faces

Shiya Li¹, Yongxuan Tan¹, Samuel Willis¹, Mohanad Bahshwan^{2,3}, Joseph Folkes¹, Livia Kalossaka¹, Usman Waheed¹, Connor Myant^{1*}

¹Dyson School of Design Engineering, Imperial College London, London, SW7 1AL, United Kingdom

²Department of Mechanical Engineering, Imperial College London, London, SW7 1AL, United Kingdom

³Department of Mechanical and Materials Engineering, University of Jeddah, Jeddah, Saudi Arabia

Abstract: Respiratory protective equipment (RPE) is traditionally designed through anthropometric sizing to enable mass production. However, this can lead to long-standing problems of low-compliance, severe skin trauma, and higher fit test failure rates among certain demographic groups, particularly females and non-white ethnic groups. Additive manufacturing could be a viable solution to produce custom-fitted RPE, but the manual design process is time-consuming, cost-prohibitive and unscalable for mass customization. This paper proposes an automated design pipeline which generates the computer-aided design models of custom-fit RPE from unprocessed three-dimensional (3D) facial scans. The pipeline successfully processed 197 of 205 facial scans with <2 min/scan. The average and maximum geometric error of the mask were 0.62 mm and 2.03 mm, respectively. No statistically significant differences in mask fit were found between male and female, Asian and White, White and Others, Healthy and Overweight, Overweight and Obese, Middle age, and Senior groups.

Keywords: Respiratory Protective Equipment; Design Automation; Mass Customization; Additive Manufacturing; 3D Graphics

*Correspondence to: Connor Myant, Dyson School of Design Engineering, Imperial College London, London, SW7 1AL, United Kingdom; connor.myant@imperial.ac.uk

Received: July 15, 2021; **Accepted:** August, 2021; **Published Online:** October 13, 2021

Citation: Li S, Tan Y, Willis S, *et al.*, 2021, Toward Mass Customization Through Additive Manufacturing: An Automated Design Pipeline for Respiratory Protective Equipment Validated Against 205 Faces. *Int J Bioprint*, 7(4):417. <http://doi.org/10.18063/ijb.v7i4.417>

1. Introduction

Respiratory protective equipment (RPE) is routinely mandated across a wide range of industries to protect millions of workers worldwide from inhaling harmful airborne particles, gases or vapors that are present in the environment. Some examples of respirator masks are disposable N95/FFP3 used in the healthcare sector, or re-usable elastomeric half-mask RPE commonly used in construction, mining, firefighting, and manufacturing. The performance of RPE depends on three factors: (i) compliance, (ii) comfort, and (iii) effective seal. The coronavirus (COVID-19) pandemic has brought the

world's attention to RPE's long-standing but often neglected problem of poor fit and its associated issues such as device-related pressure ulcers. High incidence (97%) of skin damage over the nasal bridge and cheeks among frontline health-care personnel wearing standard-sized RPE has been reported as a serious occupational hazard^[1]. These skin damages are likely caused by excessive strap pressure applied on poorly fitted masks to improve seal at the skin/mask interface^[2]. Excessive strap pressure can result in user discomfort, which is often cited as a major factor for non-compliance^[3]. Thus, improving fit will improve the effectiveness of RPE across all three success factors.

Users must pass a fit test to ensure an effective seal is achieved before they are deployed in high-risk environment. Despite its importance, there is clear evidence that current commercially available disposable RPE^[4] or reusable elastomeric RPE^[5] are inadequate at creating an effective seal for all demographic user groups. There are numerous reports of demographic bias in RPE fit test failure rates. It has been found that female users were nearly twice as likely to fail a fit test compared to male users^[6-10]. Fit test failure rates were also found to be skewed across different ethnic groups. Asian users have failure rate as high as 54%^[11] and African users at 86%^[12] as compared to about 5 – 10% among Caucasian users^[7,8,13]. Other than gender and ethnicity, age has also been reported as another factor that affects fit test failure rate^[14]. More importantly, it was found that certain combination of subdemographic groups will lead to a higher fit test failure rate. For example, McMahon *et al.*^[7] reported statistical significant difference ($P < 0.05$) in fit test passing rates among age groups in women (19 – 71 years old with an average 10 years increment for each age group), but not in men. Sandkovsky *et al.*^[15] also found that only females with body mass index (BMI) >25 are at higher risk of failing a fit test, but not males.

These demographically biased fit test failure rates are potentially caused by the limitations associated with design methodologies employed for mass producing wearables. The conventional design method is based on anthropometric sizing, which are anthropometric surveys that collect body dimensions from a sample population and statistically analyze them to suggest a sizing system (e.g. three-size system that consists of small, medium, and large) to cover majority of the population^[16,17]. For RPE masks, respirator fit test panels (two-Dimensional charts) are typically developed from analyzing 1-Dimensional facial dimensions collected from thousands of subjects to provide an objective tool for selecting a few representative human test subjects based on their facial characteristics for use in research, product development, testing, and certification^[18]. The panel is built with the aim to cover about 95% facial variation of a population and can be segmented into a few broad categories to inform a sizing system to guide the design of RPE. One of the earliest and most referenced respirator fit test panels was developed based on bivariate distribution of face length and lip length (for half-face piece RPE) or face length and face width (for full-face piece RPE) data from an anthropometric survey of 4000 male subjects in the US Air Force by Los Alamos National Laboratory^[19] in the early 1970s. Recently in 2007, the National Institute for Occupational Safety and Health (NIOSH) recognized the unsuitability of using outdated military data for the design of civilian RPE, and developed a new fit test panel using data (3997 subjects) from a 2001 anthropometric survey of civilian respirator

users^[20]. Despite having a more updated dataset, several large-scale comparative anthropometric studies have reported statistically significant differences ($P < 0.05$) in key face dimensions (e.g. face width, length, and nose protrusion) between males and females, different ethnic groups (Asian, White, African, Hispanic, etc.), and age groups (18 – 29 years old and above 45 years old)^[21-24] in the updated panel. Respirator manufacturers may create different product sizes based on demographic-specific anthropometric sizing to accommodate such differences. However, each additional size will incur additional tooling costs for mass production, therefore making it economically undesirable. The anthropometric sizing-based design methodology was developed decades ago to enable affordable mass customization (MC) of wearables through conventional mass production methods, such as injection molding, and it had been shown to result in design bias toward certain demographic groups and higher failure rates in protective equipment as mentioned above. With the maturation of advanced manufacturing techniques such as additive manufacturing (AM) which can create custom-fit product at near-zero tooling cost, it is time to re-think and develop new design methods to facilitate the use of such new manufacturing methods to provide well fitted masks for people from all backgrounds, regardless of their gender, ethnicity, age, or BMI.

AM has been identified as the next generation agile manufacturing system that enables the MC of custom-fit products^[25-29]. A key strength of AM is its near-zero tooling cost associated with every new design, which greatly reduces the per part manufacturing cost as compared to mass production processes such as injection molding. AM has been widely adopted to produce custom-fit products including traditionally custom-made medical devices such as maxillofacial prosthetics^[30-32], foot orthosis^[33,34], removable partial denture^[35], or mass-produced ergonomic products such as shoe insoles^[36,37], and aircrew seats^[25]. In recent years, AM has been explored to produce custom-fit specialty masks, such as Bi-level/Continuous Positive Airway Pressure (BiPAP/CPAP) masks^[38-40], where they have been shown to have less leakage and better comfort as compared to conventional generically designed masks. For RPE, custom-fit face seals have been shown to distribute contact pressure more evenly across the contact area, reducing the occurrence of high pressure imposed by commercial mass-produced RPE masks on areas such as the nose bridge, upper cheek, middle cheek and lower cheek and chin^[41]. There are also ongoing investigations on whether three-dimensional (3D) printed tailored RPE can improve fit test passing rate and provide better sustained comfort than conventional RPE^[42,43]. AM can also serve as an agile supply chain solution during an emergent public health crisis^[44-48]. During the earlier days of the COVID-19 pandemic, various government

agencies, local communities, and individual makers have used AM as a supply chain response to de-centralize production and combat supply chain disruption for RPE and other protective equipment^[48-57].

Despite the promises of AM in producing custom fit RPE, major cost barriers exist in adopting AM for large-scale production. One key cost contributor stems from a highly manual and time-consuming customization process, which can add up to 20 – 30% of the overall AM production cost^[25,34,37,58]. Sporadic efforts have been made over the past few decades to simplify and shorten the AM design process. The most utilized method has been parametric geometric modeling, where a generic parametric computer-aided design (CAD) model is created with control points that can be automatically updated based on the shape of an input scan. Such approach has been applied to customizable medical devices, such as protective face masks, wrist splints, ankle-foot orthotics^[59,61], and recently to BIPAP/CPAP masks^[38,40]. However, these are semi-automated modeling processes where a technician with CAD modeling knowledge is needed to perform manual operations such as aligning the generic model to a raw scan. Studies demonstrating a fully automated customization process for traditionally mass-produced body-fitted products are rare. Ellena *et al.*^[62] proposed a design process for customizing bicycle helmets, where a statistical shape model was utilized to classify a head scan into one out of four helmet sizes before cropping away the inner lining of the helmet with a generic B-Spline head surface adapted to the shape of the head scan using an iterative genetic algorithm^[63]. While it is a fully automated process, it essentially uses a sizing-based approach where the statistical shape model was built by analyzing 222 head scans that may be representative of the Australian cyclist population, but not other demographic groups. For RPE designs, the sample size required could be much larger (e.g. the US NIOSH panel used almost 4000 subjects) for a particular demographic group. The amount of resources and time needed to collect a large-scale 3D anthropometric database and to build a statistical shape model for each applicable demographic group defeats the purpose of lowering design cost for tailor-fit products. Sela *et al.*^[64] proposed a fully automated pipeline to generate customized CPAP masks based on a 3D scan or depth image of a person's face. The shape of the mask model was customized by updating 256 control points on a generic mask model made up with Non-uniform Rational Basis Spline (NURBS) surfaces. However, automatically deforming a generic NURBS-based geometric model with organic shape can be problematic, particularly given the complexity and high variability of facial shapes. The pipeline was only validated against one subject; therefore, its robustness against a larger dataset remains unknown.

To the best of authors' knowledge, there has not been a study demonstrating a completely automated process for customizing respirator masks and validated against a 3D face dataset.

Recently, the authors^[65] proposed a new automated respirator mask customization process which reduced design time from hours to minutes. While it is a promising pipeline, the pipeline has yet to be seamlessly integrated, neither has it been validated against a reasonable dataset. This study builds upon this previous work^[65] and integrates a CAD Application Programming Interface (API) with the rest of the pipeline to present a seamless and automated design pipeline for generating custom-fitted respirator masks ready to be manufactured using AM techniques.

To investigate whether this pipeline can be universally applied to people from different demographic backgrounds, an online portal was created to recruit participants during the COVID-19 lockdown periods in the UK, where their facial scans and demographic information were collected. Success rate, computational run time, and fit (how well a mask fits to a face) were evaluated. Furthermore, fit results were compared across subcategories of demographics to investigate whether the pipeline can produce respirator mask models that fit equally well to people across different age (young, middle aged, senior), gender (male or female), ethnic (Asian, White, and Others), or BMI groups (healthy, overweight, and obese).

2. Methods

2.1. RPE design pipeline

An automated MC design pipeline, shown in **Figure 1**, was employed for this study. This pipeline is based on our previous study which employs a series of alignment and template fitting processes^[65] to represent user-submitted 3D facial scans using a universal 3D face template mesh. This removes heterogeneity across different raw facial meshes in terms of orientation, location, and mesh structure (vertex indexing and triangulation), thereby enabling the subsequent automatic extraction of topographical data from a large facial dataset. Using a set of predefined vertices on the template mesh as landmarks, 200 points on two egg-shaped loops based on those landmark locations were projected onto the fitted template

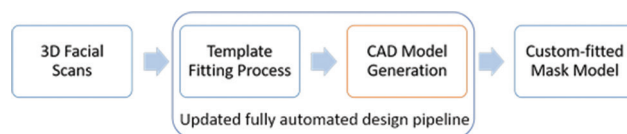


Figure 1. Pipeline overview, the computer-aided design model generation step (highlighted) is now integrated into the design pipeline.

mesh, forming the contact region between the mask and the user's face, greater details can be found in Li *et al.*^[65]. These points together with the set of landmarks act as the reference geometry in the CAD model generation step.

In the previous study^[65], Autodesk Fusion 360 API was employed. However, as it cannot be readily integrated with the rest of the pipeline which was written in MATLAB, a Python based Blender script is now utilized to seamlessly interface the CAD API into the pipeline such that the whole pipeline can run in a headless mode. Blender builds polygonal 3D models from successive addition of vertices, edges, and faces through functions with defined rules and constraints. This polygon-based generative geometric modeling approach can robustly handle the complexity and high variation of facial topographies, particularly around the nasal regions, making it well suited to the requirements of a MC pipeline for RPE. The design of the respirator mask (**Figure 2**) remained the same^[65] with three standard components (grey) and a modifiable component (blue) that will be updated geometrically in blender to achieve custom-fit.

2.2. Participants

Participants were recruited from mid-July 2020 to mid-October 2020. Due to travel restrictions during the COVID-19 pandemic, a dedicated online portal^[66] was created to collect 3D facial scans remotely. This way of data collection transcends geographical boundaries, thereby enabling us to reach a wider demographics. Recruitment was advertised on mainstream media platforms such as the BBC^[67], as well as on various social media platforms. As a token of appreciation to each participant, a custom-fitted mask model generated from the pipeline was emailed to the participant with

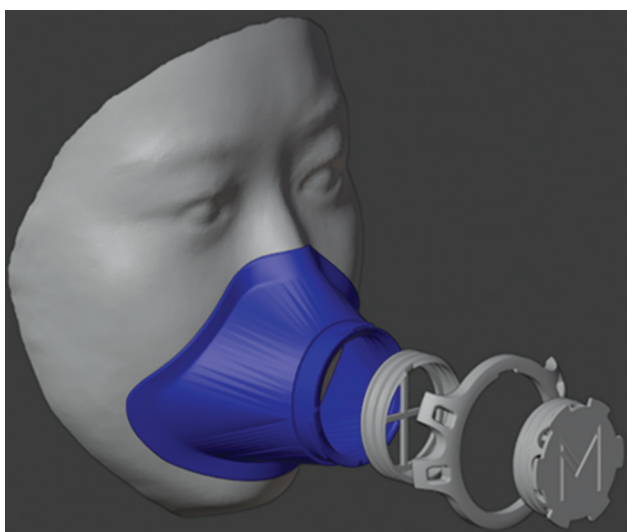


Figure 2. Custom-fitted mask body generated using Blender with standard FFP3 filter components.

assembly and manufacturing instructions so that he/she can manufacture the mask at home (if a 3D printer is available) or through commercial 3D printing services. This also served as a supply chain response to the global mask shortage at that time, as the 3D printed mask could be used as a face covering or face shield.

As facial scans are sensitive biometric data, Data Protection Impact Assessment has been carefully conducted and approved by Imperial College London to ensure all data-associated activities, including online data collection, transfer, storage, and analyses, are secure and compliant with relevant data protection regulations. The study protocol (19IC5167) was approved by the Science Engineering Technology Research Ethics Committee, Imperial College London.

Eligible participants were adults (≥ 18 years) regardless of gender, ethnicity, or BMI. Before scanning, participants were asked to read through a Participant Information Sheet to understand the project, how their data will be utilized and to clarify any questions. Written instructions^[68] were also provided on the online portal to instruct participants to prepare for scanning by doing the followings: clean shave their face, remove any glasses, and pin/tie all hair if it is obstructing the face. Video instructions^[68] were provided to ensure that facial data were acquired under the same conditions. Participants were recommended to use an iPhone X or newer versions (Apple Inc., Cupertino, California, USA) with a TrueDepth camera to acquire their facial scans. However, facial scans obtained from other acquisition devices were also accepted. If an iPhone was used, software applications recommended for creating and exporting 3D facial scans were ScandyPro (Scandy, New Orleans, USA) and Bellus3D (Bellus3D, Campbell, California, USA). Participants were also instructed to remain in a neutral expression during the data acquisition process. Once a scan had been acquired, participants were instructed to upload their scans through the online portal. Demographic information including age, gender, ethnicity, weight, and height were collected through a short survey in the submission process. Before the final submission, permission was sought from each participant to use their data anonymously through an Adult Consent Form. Details of the survey and consent form can be found in the online portal^[69].

2.3. Scan exclusion

Facial data acquisition is not a trivial task and will require the user to have a good level of understanding of the acquisition device and software to obtain 3D facial data with minimal noise and obstruction. While written and video instructions were provided to guide the participants on data acquisition, it cannot be assumed that all participants have followed the instructions diligently

and were able to produce good quality scans. Therefore, each scan was manually checked against the following set of exclusion criteria to ensure that all scans were of similar quality before submitted to the pipeline:

- i. Being duplicates, that is, having two or more submissions containing the same face
- ii. Having any obstruction on the face that may interfere with the mask, including beard, moustache, glasses, and piercing.
- iii. Having poor quality, including poor reconstruction of facial geometry, corrupted file, scan resolution at >0.5 mm
- iv. Having been modified by the participant to remove any holes/defects
- v. Having non-neutral facial expression
- vi. Not human faces, that is, scans of other objects
- vii. Being manifold, that is, enclosed to form a solid volume, instead of being an open surface

A total of 322 submissions were received at the end of recruitment, of which 117 were excluded based on the above criteria. **Figure 3** shows a summary of the excluded scans.

2.4. Computational time evaluation

All 205 included scans were processed through the pipeline on a remote Linux workstation (Intel® XEON®

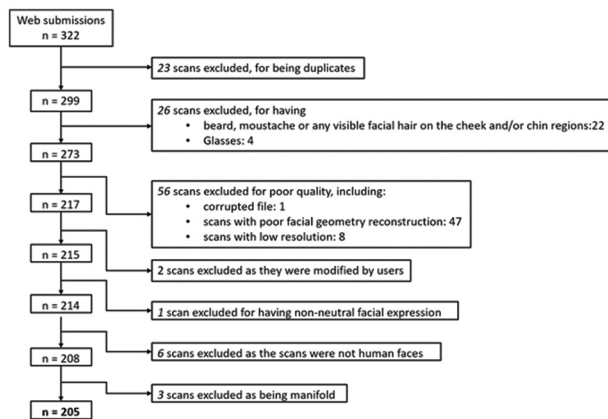


Figure 3. Facial scans exclusion.

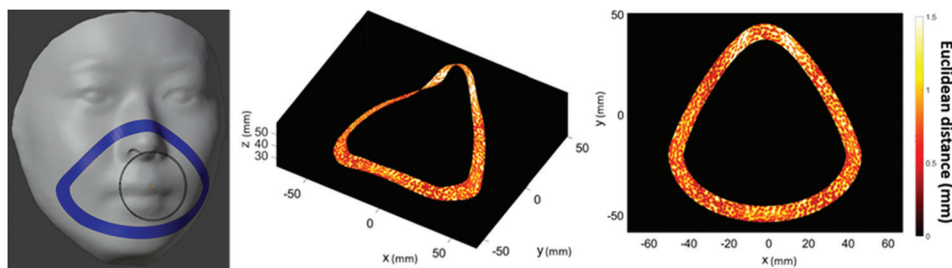


Figure 4. Euclidean distance between mask surface and a aligned face scan.

4114 2.2 2400MHz 10-Core CPU, 256 GB DDR4 2666 DIMM Memory, Nvidia Quadro P1000 4GB GFX). For each input scan, a solid respirator mask CAD model was generated by the pipeline described in Section 2.1. The total run time for processing a scan and generating a CAD model was recorded.

2.5. Fit evaluation

Euclidean distance was used to computationally evaluate fit between the mask surface and the aligned face mesh (**Figure 4**). A nearest neighbor search^[70] was performed through a space-partitioning method called K-dimensional tree^[71] to pair each vertex on the mask surface with its nearest neighboring vertex on the aligned mesh. The nearest neighbor search was defined as: given a set of points $u \in U$ (the aligned mesh), and a set of query points $v \in V$ (the mask surface), for all v , find the closest points to U . The Euclidean distance was computed for each closest pair. Subsequently, the maximum and root mean square error (RMSE) of the Euclidean distances of were computed. The Maximum Euclidean distance indicates the maximum gap between a mask and its corresponding face mesh, whereas the RMSE Euclidean distance indicates the average gap between the mask and the face.

Maximum and RMSE Euclidean distance results were grouped into age, gender, ethnicity, and BMI subcategories according to demographic data reported by participants. For age, results have been grouped into three subcategories: Young (18 – 39 years old), Middle aged (40 – 54 years old), and Seniors (55 years old and above). There is not an international standard on age classification according to craniofacial shape change; however, various studies have shown evidence of craniofacial change as a result of aging^[72-75]. Therefore, it is important to investigate whether the current pipeline can deliver similar fit results across different age groups. Age has generally been grouped into three categories (young, middle aged, and senior), and the cutoff points are approximately 15 – 25, 35 – 45, and 55 – 65 years old. In this study, the author, therefore, used 18 – 39 years old for young adults, 40 – 54 years old for middle aged adults, and 55 years and above for seniors. For gender, results were grouped into male and female categories. BMI grouping was based on the

standard adult BMI classification^[76]: underweight (BMI < 18.5), healthy (18.5 < BMI ≤ 24.9), overweight (25.0 < BMI < 29.9), and obese (BMI > 30.0). For ethnicity, participants were grouped into the broad categories of Asian, White, and Others (including Black, Arabs, and any other ethnicity) as reported by participants.

3. Results and discussion

Using our pipeline, 197 of the 205 included scans returned a valid CAD model and 8 scans were rejected by the alignment checking algorithms in the pipeline (misalignment between input scan and template mesh), which gives an overall processing success rate of 96.1%. **Table 1** shows the respective average run time for the processed 197 scans obtained from Bellus3D, ScandyPro and Lightstage. Compared to a manual process the pipeline has achieved significant time-savings. The average run time for processing a single scan was <2 min (104.4) that a significant portion of which time was consumed by the template fitting sub-process. The underlying code for this sub-process has not been optimized for the graphics processing unit (GPU) computation; hence, further time savings may be attained through GPU rather than CPU computation. This is a significant improvement from earlier manual process studies. This time saving is crucial to scale up the production for mass-customizing respirator masks, which has a much higher demand than conventionally customized orthotics or prosthetics. In addition, the customisation process is now completely automated which eliminates labor cost. Cazon *et al.*^[61] have reported that labor cost can take up to 80% of the entire AM design cost; therefore, such savings is significant for making AM a more viable production method for the MC of respirator masks. Notably, the average run time per scan for ScandyPro scans was the longest (at almost 4 min/scan) compared to Bellus3D (<1 min/scan) and Light stage scans (<1.5 min/scan). This extended runtime is owed to the fact that ScandyPro scans contained significantly greater number of vertices than the other two. In addition, the ScandyPro scans included noisier data, including large neck/shoulder parts and many disconnected regions scattered around the face. Collectively, these resulted in longer time to perform the template fitting process.

Table 2 shows participants' profiles grouped into the demographic categories, and their corresponding Maximum and RMSE Euclidean distances. The majority

Table 1. Average run time.

Acquisition method	Average run time, mean (sd)
All	104.4 (95.2)
Bellus3D	52.5 (25.7)
ScandyPro	235.5 (89.9)
Lightstage	133.3 (56.8)

of the participants were male (80.7%), or White (76.1%), or having BMI more than 25 (85.8%). The average RMSE Euclidean distance between a mask surface and a face is 0.62 ± 0.20 mm (mean \pm sd) for all 197 scans. This means that the mask model was able to achieve an average sub-millimeter accuracy. The Maximum Euclidean distance is 2.03 ± 0.75 mm (mean \pm sd), located on nasal sidewalls. Lee *et al.*^[77] used a virtual fit testing method on 3D facial data of 336 Korean Air Force men and found that the gap between a pilot oxygen mask (similar to a reusable elastomeric half-face respirator) at the nasal bridge is approximately 6 mm when pressing the mask tightly onto a face (10 mm into the cheek). A maximum 2 mm gap at the nasal sidewalls instead of the nasal bridge, which has been reported as the most commonly injured site for respirator users^[1], is a significant improvement from the mass-produced RPE. In addition, contrary to the design bias in current commercially available RPE, where fit was poorer among females and Asians, the Maximum Euclidean distance was slightly lower for females (1.82 mm) as compared to males (2.08 mm), and Asians (1.80 mm) as compared to the others (White: 2.05 mm and others: 2.33 mm).

To investigate if the proposed pipeline could produce respirator masks that fit equally well to people with different demographic backgrounds, the following hypothesis was tested: there will be no difference between the maximum or RMSE Euclidean distance across each subcategory under age, gender, ethnicity or BMI. Choice of an appropriate statistical test is dependent on the nature of the Euclidean distance results. Before deciding on an appropriate statistical test, Shapiro–Wilk tests were conducted to check for normality of the distributions for each grouped RMSE and maximum Euclidean distances. Most of the demographic groups rejected the null hypothesis ($P < 0.05$) that the data is normally distributed with unspecified mean and variance, except for the Maximum Euclidean Distance in Female group ($P = 0.12$), RMSE Euclidean distance in Other Ethnicity group ($P = 0.31$), and RMSE Euclidean distance in Healthy BMI group ($P = 0.23$). Nonetheless, for these groups, the sample size is small (≤ 30). Therefore, the nonparametric Wilcoxon Rank Sum Test (confidence level at 95%) was used to compare outcomes between each pair of subcategories in age, gender, ethnicity and BMI. The underweight group was excluded as the sample size is too small ($n = 1$).

Wilcoxon Rank Sum test results (**Table 3**) showed that there is no statistically significant difference for RMSE and maximum Euclidean distances between Male and Female, Asian and White, White and others, healthy and overweight, overweight and obese, Middle age, and senior groups. This suggests that the pipeline produced mask models that fit equally well across these groups. This

Table 2. Participants' profile and Euclidean distance results.

	Total (n=197)	RMSE Euclidean distance (mm), mean (sd)	Maximum Euclidean distance (mm), mean (sd)
Overall		0.62 (0.20)	2.03 (0.75)
Gender, <i>n</i> (%)			
Male	159 (80.7)	0.62 (0.20)	2.08 (0.77)
Female	30 (15.2)	0.64 (0.21)	1.82 (0.61)
No response	8 (3.1)	-	-
Ethnicity, <i>n</i> (%)			
Asian	27 (13.7)	0.59 (0.18)	1.80 (0.62)
White	150 (76.1)	0.62 (0.20)	2.05 (0.75)
Others	14 (7.1)	0.63 (0.24)	2.33 (0.86)
No response	6 (3.1)	-	-
BMI, mean (sd)			
Underweight (<18.5)	-(0.5)	-	-
Healthy (18.5 – 24.9)	23.1±1.8 (10.7)	0.59 (0.17)	1.76 (0.67)
Overweight (25.0 – 29.9)	27.4±1.3 (42.1)	0.61 (0.19)	2.02 (0.70)
Obese (>30.0)	36.6±9.3 (43.7)	0.64 (0.21)	2.12 (0.79)
No response	-(3.0)	-	-
Age, mean (sd)			
Young (18 – 39)	29.3±6.3 (30.5)	0.56 (0.20)	1.71 (0.64)
Middle aged (40 – 54)	48.5±4.1 (33.5)	0.62 (0.18)	2.06 (0.72)
Senior (55 and above)	61.3±5.3 (32.5)	0.68 (0.20)	2.32 (0.75)
No response	-(3.6)	-	-

BMI; Body mass index, sd; Standard deviation

Table 3. Wilcoxon Rank Sum test results.

Category 1	Category 2	RMSE Euclidean Distance (mm)		Maximum Euclidean distance (mm)	
		H	P value	H	P value
Gender					
Male	Female	0	0.814	0	0.061
Ethnicity					
Asian	White	0	0.375	0	0.061
Asian	Others	0	0.711	1	0.035
White	Others	0	0.941	0	0.120
BMI					
Healthy	Overweight	0	0.740	0	0.100
Healthy	Obese	0	0.580	1	0.035
Overweight	Obese	0	0.673	0	0.394
Age					
Young	Middle age	0	0.078	1	0.002
Young	Senior	1	0.005	1	0.000
Middle age	Senior	0	0.165	0	0.051

is a significant improvement compared to conventional anthropometric sized RPE where failure rates were found to be as high as double among females compared to male colleagues^[6-8], or 16% – 54% among Asians^[11,13]. The same analyses have been conducted for just the Bellus3D

scans and just the ScandyPro scans respectively (Light stage scans were not used due to its small sample size), and similar results were found. This shows that the pipeline can produce demographically non-biased mask models regardless of acquisition methods.

There are statistically significant differences between the Young and the Senior groups for RMSE Euclidean distance, and between the Asian and Others, Healthy and Obese, Young and Middle-age, and Young and Senior for Maximum Euclidean distance. Nonetheless, all differences in their absolute values (**Table 2**) were <1 mm. The Maximum Euclidean distance is 1.7 mm – 2.3 mm for each of these groups, which are significantly smaller than the 6 mm gap reported in similar commercial masks^[78]. With a much smaller gap to fill, users can potentially apply less strap pressure onto the mask to create a good seal, reducing chances of skin trauma.

This study may be under-powered as the current sample is skewed towards male, White, and high BMI populations, whereas the sample size for female, non-White and normal BMI populations were small. Future studies should look to collect a more evenly distributed gender, BMI and ethnicity sample with a larger sample size to further validate the universality of this pipeline. Nonetheless, initial results show great potential to produce customized RPE products that can fit equally well across different demographic and demographic subgroups. This contrasts current anthropometric sizing methodologies which contain inherent biases due to the sample populations they were based on.

The proposed pipeline was deployed as an online application which promoted decentralized manufacturing during the period when there was a global shortage of RPE. However, the pipeline's main contribution is to quickly create custom-fitted RPE models that offer superior fit to commercial masks, making it a viable tool to produce RPE products in the healthcare and construction industry where good fit and comfort are required. This pipeline can be deployed quickly in the extent of future pandemics.

The pipeline was validated computationally to demonstrate that it is possible to rapidly produce RPE design models that fit well to a user's face. The pipeline offers a route to lower product unit costs by automating the design phase, thus removing that barrier for mass customizing wearables. It also shows a novel and promising design methodology that is not inherently biased towards specific demographic group as it is in the traditional anthropometric sizing approach. The mask model presented in this pipeline had been shown to be successfully fabricated through the stereolithography (SLA) process in our previous study^[65], taking an average of 8 h and using 40 mL of resin to fabricate the mask body. A fit test study is currently being conducted to evaluate the performance of the 3D printed custom-fitted masks against commercial masks. Future studies can build upon our previous and current work to investigate other factors affecting the manufacturing of the mask, including the impact of different AM build processes, such as SLA, fused deposition modeling and selective

laser sintering, and post-processing techniques on the surface finish of the mask/face contact area, and Young's Modulus, biocompatibility and sterilizability of the print materials. Different filter materials with different levels of particle filtration capabilities can also be evaluated to Filter materials, with different levels of particle filtration capabilities, can also be investigated to determine their performance and impact on custom fitted masks.

4. Conclusions

This study presented a fully automated design pipeline to enable MC of RPE via AM. The pipeline was validated against 205 facial scans to generate custom fit respirator mask CAD models. The pipeline achieved 96% processing success rate with <2 min/scan processing time. When virtually fitted, the mean RMSE and Maximum Euclidean distance between the masks and faces were 0.62 mm and 2.03 mm, respectively. It was found that there was no statistically significant difference in goodness of fit between different age, gender, ethnicity, and BMI subgroups. When combined with appropriate AM processes and materials, it could be a promising route towards the true MC of RPE or even other body-fitted products.

Acknowledgments

The authors would like to thank Lara Lewington and the team from the BBC, and Kristie Lu Stout from the CNN, for featuring this study - the Mensura Mask project. These media exposures have greatly helped us with volunteer recruitment around world so that we can build a dataset with better demographic distribution. The authors would also like to thank Mike Westlake from the Autodesk for connecting us with the CNN. Finally, the authors would like to thank all volunteers who have participated in this study.

Funding

This work was funded by Community Jameel and Imperial College London under the award of the Community Jameel Imperial College COVID-19 Excellence Fund, and the Imperial College President's PhD Scholarship Fund.

Conflicts of interest

The authors declare no conflict of interest.

References

1. Lan J, Song Z, Miao Z, *et al.*, 2020, Skin Damage among Health Care Workers Managing Coronavirus Disease-2019. *J Am Acad Dermatol*, 82:1215-6.
2. Gefen A, Alves P, Ciprandi G, *et al.*, 2020, Device-related

- Pressure Ulcers: SECURE Prevention. *J Wound Care*, 29:S1-52.
3. Gosch, M.E., Shaffer RE, Eagan AE, et al., 2013, B95: A New Respirator for Health Care Personnel. *Am J Infect Control*, 41:1224-30.
 4. O’Kelly E, Arora A, Pirog S, et al., 2021, Comparing the Fit of N95, KN95, Surgical, and Cloth Face Masks and Assessing the Accuracy of Fit Checking. *PLoS One*, 16:e0245688. <https://doi.org/10.1371/journal.pone.0245688>
 5. Pompeii LA, Kraft CS, Brownsword EA. et al. Training and Fit Testing of Health Care Personnel for Reusable Elastomeric Half-Mask Respirators Compared With Disposable N95 Respirators. *JAMA*, 323:1849-52. <https://doi.org/10.1001/jama.2020.4806>
 6. Han DH, Choi KL, 2003, Facial Dimensions and Predictors of Fit for Half-mask Respirators in Koreans. *Aiha J*, 64:815-22. <https://doi.org/10.1080/15428110308984877>
 7. McMahon E, Wada K, Dufresne A, 2008, Implementing Fit Testing for N95 Filtering Facepiece Respirators: Practical Information from a Large Cohort of Hospital Workers. *Am J Infect Control*, 36:298-300. <https://doi.org/10.1016/j.ajic.2007.10.014>
 8. Ascott A, Crowest P, de Sausmarez E, et al., 2020, Respiratory Personal Protective Equipment for Healthcare Workers: Impact of Sex Differences on Respirator Fit Test Results. *Br J Anaesth*, 126:e48-e49. <https://doi.org/10.1016/j.bja.2020.10.016>
 9. Regli A, Sommerfield A, von Ungernd.org/10.1 B, 2021, The Role of Fit Testing N95/FFP2/FFP3 Masks: A Narrative Review. *Anaesthesia*, 76:91-100. <https://doi.org/10.1111/anae.15261>
 10. Lam S, Lee JK, Yau SY, et al., 2011, Sensitivity and Specificity of the User-seal-check in Determining the Fit of N95 Respirators. *J Hosp Infect*, 77:252-256. <https://doi.org/10.1016/j.jhin.2010.09.034>
 11. Yu Y, Jiang L, Zhuang Z, et al. 2014, Fitting Characteristics of N95 Filtering-facepiece Respirators Used Widely in China. *PLoS One*, 9:e85299. <https://doi.org/10.1371/journal.pone.0085299>
 12. Spies A, Wilson KS, Ferrie R, 2011, Respirator Fit of a Medium Mask on a Group of South Africans: A Cross-sectional Study. *Environ Health*, 10:1-7. <https://doi.org/10.1186/1476-069x-10-17>
 13. Wilkinson IJ, Pisaniello D, Ahmad J, et al., 2010, Evaluation of a Large-scale Quantitative Respirator-fit Testing Program for Healthcare Workers: Survey Results. *Infect Control Hosp Epidemiol*, 31:918-25. <https://doi.org/10.1086/655460>
 14. Zhuang Z, Bergman M, Brochu E, et al., 2016, Temporal Changes in Filtering-facepiece Respirator Fit. *J Occup Environ Hyg*, 13:265-74.
 15. Sandkovsky U, Schwedhelm M, Grayer S, et al., 2017, Small changes make a big difference in the fit of N95 respirators. *Open Forum Infect Dis*, 4:S166. <https://doi.org/10.1093/ofid/ofx163.292>
 16. Roebuck JA, 1995, Anthropometric Methods: Designing to Fit the Human Body. In: Human Factors and Ergonomics Society. Santa Monica, California: Humanoid Factors and Ergonomics Society. <https://doi.org/10.1177/106480469500300309>
 17. Pheasant S, 2014, Bodyspace: Anthropometry, Ergonomics and the Design of Work: Anthropometry, Ergonomics and the Design of Work. Boca Raton, Florida: CRC Press. <https://doi.org/10.1201/9781482272420>
 18. Chen W, Zhuang Z, Benson S, et al., 2009, New Respirator Fit Test Panels Representing the Current Chinese Civilian Workers. *Ann Occup Hyg*, 53:297-305. <https://doi.org/10.1093/annhyg/men089>
 19. Hack A, Hyatt EC, Held BJ, et al., 1973, Selection of Respirator Test Panels Representative of US Adult Facial Sizes. New Mexico: Los Alamos Scientific Lab., N. Mex, (USA). <https://doi.org/10.2172/4335046>
 20. Zhuang Z, Bradtmiller B, 2005, Head-and-Face Anthropometric Survey of US Respirator Users. *J Occup Environ Hyg*, 2:567-576. <https://doi.org/10.1080/15459620500324727>
 21. Zhuang Z, Landsittel D, Benson S, et al., 2010, Facial Anthropometric Differences among Gender, Ethnicity, and Age Groups. *Ann Occup Hyg*, 54:391-402.
 22. Kim H, Han DH, Roh YM, et al., 2003, Facial Anthropometric Dimensions of Koreans and their Associations with Fit of Quarter-mask Respirators. *Ind Health*, 41:8-18. <https://doi.org/10.2486/indhealth.41.8>
 23. Du L, Zhuang Z, Guan H, et al., 2008, Head-and-face Anthropometric Survey of Chinese Workers. *Ann Occup Hyg*, 52:773-782.
 24. Yang L, Shen H, Wu G, 2007, Racial Differences in Respirator Fit Testing: A Pilot Study of Whether American Fit Panels are Representative of Chinese Faces. *Ann Occup Hyg*, 51:415-421. <https://doi.org/10.1093/annhyg/mem005>
 25. Tuck CJ, Hague RJ, Ruffo M, et al., 2008, Rapid Manufacturing Facilitated Customization. *Int J Comput Integr Manufact*, 21:245-258. <https://doi.org/10.1080/09511920701216238>
 26. Tan HW, An J, Chua CK, et al., 2019, Metallic Nanoparticle Inks

- for 3D Printing of Electronics. *Adv Electron Mater*, 5:1800831. <https://doi.org/10.1002/aelm.201800831>
27. Choong YY, Maleksaeedi S, Eng H, *et al.*, 2020, High Speed 4D Printing of Shape Memory Polymers with Nanosilica. *Appl Mater Today*, 18:100515. <https://doi.org/10.1016/j.apmt.2019.100515>
 28. Tan HW, Saengchairat N, Goh GL, *et al.*, 2020, Induction Sintering of Silver Nanoparticle Inks on Polyimide Substrates. *Adv Mater Technol*, 5:1900897. <https://doi.org/10.1002/admt.201900897>
 29. Ng WL, Chua CK, Shen YF, 2019, Print me an Organ! Why we are not there yet. *Prog Polym Sci*, 97:101145. <https://doi.org/10.1016/j.progpolymsci.2019.101145>
 30. Bibb R, Eggbeer D, Evans P, 2010, Rapid Prototyping Technologies in Soft Tissue Facial Prosthetics: Current State of the Art. *Rapid Prototyp J*, 16:25852. <https://doi.org/10.1108/13552541011025852>
 31. Eggbeer D, Evans PL, Bibb R, 2006, A Pilot Study in the Application of Texture Relief for Digitally Designed Facial Prostheses. *Proc Inst Mech Eng Part H*, 220:705-14. <https://doi.org/10.1243/09544119jeim38>
 32. Kai CC, Meng CS, Ching LS, *et al.*, 2000, Facial prosthetic model fabrication using rapid prototyping tools. *Integr Manuf Syst*, 11:42-53. <https://doi.org/10.1108/09576060010303668>
 33. Pallari J, Dalgarno K, Munguia J, *et al.* 2010, Design and Additive Fabrication of Foot and Ankle-foot Orthoses. In: Proceedings of the 21st Annual International Solid Freeform Fabrication Symposium an Additive Manufacturing Conference. https://doi.org/10.32656/2018_29sff_symposium
 34. Pallari JH, Dalgarno KW, Woodburn J, 2001, Mass Customization of Foot Orthoses for Rheumatoid Arthritis Using Selective Laser Sintering. *IEEE Trans Biomed Eng*, 57:1750-6. <https://doi.org/10.1109/tbme.2010.2044178>
 35. Eggbeer D, Bibb R, Williams R, 2005, The Computer-aided Design and Rapid Prototyping Fabrication of Removable Partial Denture Frameworks. *Proc Inst Mech Eng Part H*, 219:195-202. <https://doi.org/10.1243/095441105x9372>
 36. Salles AS, Gyi DE, 2013, Delivering Personalised Insoles to the High Street Using Additive Manufacturing. *Int J Comput Integr Manuf*, 2013. 26:386-400. <https://doi.org/10.1080/0951192x.2012.717721>
 37. Salles AS, Gyi DE, 2012, The Specification of Personalised Insoles Using Additive Manufacturing. *Work*, 41:1771-4. <https://doi.org/10.3233/wor-2012-0383-1771>
 38. Wu YY, Acharya D, Xu C, *et al.*, 2018, Custom-Fit Three-dimensional-printed BiPAP Mask to Improve Compliance in Patients Requiring Long-term Noninvasive Ventilatory Support. *J Med Dev*, 12:0310031-8. <https://doi.org/10.1115/1.4040187>
 39. Ma Z, Hyde P, Drinnan M, *et al.*, 2021, Custom Three-Dimensional-Printed CPAP Mask Development, Preliminary Comfort and Fit Evaluation. *J Med Dev*, 15:024501. <https://doi.org/10.1115/1.4050201>
 40. Martelly E, Rana S, Shimada K, 2021, Design and Fabrication of Custom-Fit BiPAP and CPAP Masks Using Three-Dimensional Imaging and Three-Dimensional Printing Techniques. *J Med Dev*, 15:024502. <https://doi.org/10.1115/1.4049981>
 41. Cai M, Li H, Shen S, *et al.*, 2018, Customized Design and 3D Printing of Face Seal for an N95 Filtering Facepiece Respirator. *J Occup Environ Hyg*, 15:226-34. <https://doi.org/10.1080/15459624.2017.1411598>
 42. Finne H, Liacouras P, Wilsnack AR, *et al.*, Custom Fit N95 Respirator Acceptability and Fit. Bethesda, Maryland, United States: Walter Reed National Military Medical Center.
 43. Stokes AA, 2021, 3DPPE: Rapid 3D Printing of Personalised Protective Facemasks and Visors to WHO Standard for Healthcare Workers Treating SARS-CoV-2 Patients.
 44. Choong YY, Tan HW, Patel DC, *et al.*, 2020, The Global Rise of 3D Printing during the COVID-19 Pandemic. *Nat Rev Mater*, 5:637-639. <https://doi.org/10.1038/s41578-020-00234-3>
 45. Sherborne C, Claeysens F, 2021, Considerations Using Additive Manufacture of Emulsion Inks to Produce Respiratory Protective Filters against Viral Respiratory Tract Infections Such as the COVID-19 Virus. *Int J Bioprint*, 7:316. <https://doi.org/10.18063/ijb.v7i1.316>
 46. Shpichka A, *et al.*, 2020, Engineering a Model to Study Viral Infections: Bioprinting, Microfluidics, and Organoids to Defeat Coronavirus Disease 2019 (COVID-19). *Int J Bioprint*, 6:302. <https://doi.org/10.18063/ijb.v6i4.302>
 47. Bishop EG, Leigh SJ, 2020, Using Large-scale Additive Manufacturing as a Bridge Manufacturing Process in Response to Shortages in Personal Protective Equipment during the COVID-19 Outbreak. *Int J Bioprint*, 6:281. <https://doi.org/10.18063/ijb.v6i4.281>
 48. Celik HK, Kose O, Ulmeanu ME, *et al.*, 2020, Design and Additive Manufacturing of Medical Face Shield for Healthcare Workers Battling Coronavirus (COVID-19). *Int J*

- Bioprint*, 6:286.
<https://doi.org/10.18063/ijb.v6i4.286>
49. Flanagan ST, Ballard DH, 2020, 3D Printed Face Shields: A Community Response to the COVID-19 Global Pandemic. *Acad Radiol*, 27:905.
<https://doi.org/10.1016/j.acra.2020.04.020>
 50. Wesemann C, Pieralli S, Fretwurst T, et al., 2020, 3-d Printed Protective Equipment during covid-19 Pandemic. *Materials*, 13:1997.
<https://doi.org/10.3390/ma13081997>
 51. Cavallo L, Marcianò A, Cicciù M, et al., 2020, 3D Printing beyond Dentistry during COVID 19 Epidemic: A Technical Note for Producing Connectors to Breathing Devices. *Prosthesis*, 2:46-52.
<https://doi.org/10.3390/prosthesis2020005>
 52. Clifton W, Damon A, Martin AK, 2020, Considerations and Cautions for Three-Dimensional-Printed Personal Protective Equipment in the COVID-19 Crisis. *3D Print Addit Manuf*, 7:97-9.
<https://doi.org/10.1089/3dp.2020.0101>
 53. Novak JI, Loy J, 2020, A Critical Review of Initial 3D Printed Products Responding to COVID-19 Health and Supply Chain Challenges. *Emerald Open Res*, 2:24.
<https://doi.org/10.35241/emeraldopenres.13697.1>
 54. Swennen GR, Pottel L, Haers PE, 2020, Custom-made 3D-printed Face Masks in Case of Pandemic Crisis Situations with a Lack of Commercially Available FFP2/3 Masks. *Int J Oral Maxillofac Surg*, 49:673-7.
<https://doi.org/10.1016/j.ijom.2020.03.015>
 55. Novak JI, Loy J, 2020, A Quantitative Analysis of 3D Printed Face Shields and Masks during COVID-19. *Emerald Open Res*, 2:42.
<https://doi.org/10.35241/emeraldopenres.13815.1>
 56. Provenzano D, Rao YJ, Mitic K, et al., 2020, Rapid Prototyping of Reusable 3D-printed N95 Equivalent Respirators at the George Washington University. *Preprints*, 2020:2020030444.
<https://doi.org/10.20944/preprints202003.0444.v1>
 57. Greig P, Carvalho C, El-Boghdadly K, et al., 2020, Safety Testing Improvised COVIDng IPersonal Protective Equipment Based on a Modified Full-odifiSnorkel Mask. *Anaesthesia*, 75:970-1.
<https://doi.org/10.1111/anae.15085>
 58. Rogers B, Bosker GW, Crawford RH, et al., 2007, Advanced Trans-tibial Socket Fabrication Using Selective Laser Sintering. *Prosthet Orthot Int*, 31:88-100.
<https://doi.org/10.1080/03093640600983923>
 59. Schrank ES, 2011, Dimensional Accuracy of Ankle-Foot Orthoses Constructed by Rapid Customization and Manufacturing Framework. *J Rehabil Res Dev*, 48:31.
<https://doi.org/10.1682/jrrd.2009.12.0195>
 60. Paterson AM, Donnison E, Bibb RJ, et al., 2014, Computer-aided Design to Support Fabrication of Wrist Splints Using 3D Printing: A Feasibility Study. *Hand Ther*, 19:102-13.
<https://doi.org/10.1177/1758998314544802>
 61. Cazon A, Aizpurua J, Paterson A, et al., 2014, Customised Design and Manufacture of Protective Face Masks Combining a Practitioner-friendly Modelling Approach and Low-cost Devices for Digitising and Additive Manufacturing: This Paper Analyses the Viability of Replacing Conventional Practice with AM Method to Make Customized Protective Face Masks. *Virtual Phys Prototyp*, 9:251-261.
<https://doi.org/10.1080/17452759.2014.958648>
 62. Ellena T, Mustafa H, Subic A, et al., 2018, A Design Framework for the Mass Customisation of Custom-fit Bicycle Helmet Models. *Int J Ind Ergon*, 64:122-33.
<https://doi.org/10.1016/j.ergon.2018.01.005>
 63. Galvez A, Iglesias A, Puig-Pey J, 2012, Iterative Two-step Genetic-algorithm-Based Method for Efficient Polynomial B-spline Surface Reconstruction. *Inf Sci*, 182:56-76.
<https://doi.org/10.1016/j.ins.2010.09.031>
 64. Sela M, Toledo N, Honen Y, et al., 2016, Customized Facial Constant Positive Air Pressure (CPAP) Masks. *arXiv*, 2016:07049.
 65. Li S, Waheed U, Bahshwan M, et al., 2021, A Scalable Mass Customisation Design Process for 3D-printed Respirator Mask to Combat COVID-19. *Rapid Prototyp J*, 27:1302-17.
<https://doi.org/10.1108/rpj-10-2020-0231>
 66. Mensura M, 2020, Mensura Mask Website. Available from: Available from: <https://www.mensuramask.com> [Last accessed on 2021 Feb 04].
 67. BBC, 2020, What is it Like to Wear a Customised Face Mask? Available from: <https://www.bbc.co.uk/programmes/p08ky38x> [Last accessed on 2021 Feb 04].
 68. Mensura M, 2020, How to Perform a Face Scan. Available from: <https://www.mensuramask.com/instructions> [Last accessed on 2021 Jun 26].
 69. Mensura M, 2020, Participate in the Study. Available from: https://imperial.eu.qualtrics.com/jfe/form/SV_8jC7fcmYEOT6aMt [Last accessed on 2021 Jun 26].
 70. Yianilos PN, 1993, Data Structures and Algorithms for Nearest Neighbor Search in General Metric Spaces. In: Proceedings of the fourth annual ACM-SIAM Symposium on Discrete algorithms.

71. Bentley, J.L., 1975, Multidimensional Binary Search Trees Used for Associative Searching. *Commun ACM*, 18:509-517. <https://doi.org/10.1145/361002.361007>
72. Richard MJ, Morris C, Deen BF, *et al.*, 2009, Analysis of the Anatomic Changes of the Aging Facial Skeleton Using Computer-assisted Tomography. *Ophthalmic Plast Reconstr Surg*, 25:382-386. <https://doi.org/10.1097/iop.0b013e3181b2f766>
73. Kahn DM, Shaw RB Jr., 2008, Aging of the Bony Orbit: A Three-dimensional Computed Tomographic Study. *Aesthet Surg J*, 28:258-64.
74. Mendelson BC, Hartley W, Scott M, *et al.*, 2007, Age-related Changes of the Orbit and Midcheek and the Implications for Facial Rejuvenation. *Aesthet Plast Surg*, 31:419-423. <https://doi.org/10.1007/s00266-006-0120-x>
75. Zadoo VP, Pessa JE, 2000, Biological Arches and Changes to the Curvilinear form of the aging Maxilla. *Plast Reconstr Surg*, 106:460-6. <https://doi.org/10.1097/00006534-200008000-00036>
76. World Health Organization. Body Mass Index BMI. Available from: <https://www.euro.who.int/en/health-topics/disease-prevention/nutrition/a-healthy-lifestyle/body-mass-index-bmi> [Last accessed on 2021 Feb 04]. https://doi.org/10.1007/springerreference_179795
77. Lee W, Kim H, Jung D, *et al.*, 2013, Ergonomic Design and Evaluation of a Pilot Oxygen Mask. In Proceedings of the Human Factors and Ergonomics Society Annual Meeting. Los Angeles, CA: SAGE Publications Sage CA. <https://doi.org/10.1177/1541931213571371>
78. Lee W, Jung D, Park S, *et al.*, 2012, Development of a Methodology to Design a Pilot Oxygen Mask Based on Virtual Fit Testing Method. In: Proceedings of the 2012 Spring Conference of the Korean Institute of Industrial Engineers.